Polym. Bull. (2011) 67:2025–2033
DOI 10.1007/s00289-011-0618-5

ORIGINAL PAPER

Effect of organic solvent on morphology and mechanical properties of electrospun syndiotactic polypropylene nanofibers

Kei Watanabe · Taiki Nakamura ·
Byoung-Suhk Kim · Ick-Soo Kim

Received: 28 March 2011 / Revised: 6 July 2011 / Accepted: 21 August 2011 /

Abstract We study the stress–strain behaviors of the electrospun sPP single nanofibers as well as nonwoven mats, which were electrospun from sPP solutions using two different solvents (decalin and cyclohexane) by electrospinning. The effects of organic solvents were explored on the morphologies and the mechanical properties of the corresponding electrospun sPP single nanofibers and nonwoven mats. It was found that the nature of organic solvents dramatically affected the surface morphologies, the circular and looping deposition of the electrospun sPP fibers, and the mechanical properties. The tensile strength of both electrospun sPP single nanofibers and nonwoven mats prepared from decalin-base solution was stronger than that of cyclohexane-base solution.

Keywords Nanofiber · Electrospinning · Syndiotactic polypropylene · Morphology · Mechanical property

Introduction

Electrospinning is a simple and cost-effective technique used to produce the nonwoven fibrous membranes composed of ultrafine fibers in the diameter range from tens of nanometers to a few microns [1–4]. There electrospun nanofibers are featured several excellent characteristics such as very large specific surface area, high porosity, and flexibility in surface functionalities, which make the polymer nanofibers to be potential candidates for a wide range of value-added

---

K. Watanabe · T. Nakamura · B.-S. Kim (✉) · I.-S. Kim (✉)
Department of Bioscience and Textile Technology, Faculty of Textile Science & Technology, Shinshu University, Nagano 386-0015, Japan
e-mail: kbsuhk@yahoo.com

I.-S. Kim
e-mail: kim@shinshu-u.ac.jp

applications for filtration, membrane separation, capacitors, battery separators, energy storage, fuel cells, protective military clothing, biosensors, wound dressings, and scaffolds for tissue engineering, etc. [5–9]. Certainly, the mechanical properties of electrospun nanofibers, related to single nanofiber strength, average nanofiber length, and nanofiber entanglement density, are crucially important role in end-use applications [5, 10], and can be also controlled by varying solution and processing parameters or postspinning treatments. In general, the mechanical properties measured using nanofibrous nonwoven mats or yarns rather than individual fibers depend strongly on fiber orientation within the material, bonding between fibers, and slip of one fiber over another. Moreover, the strength of such nanofibrous nonwoven mats cannot be accurately calculated due to the difficulty in measuring the cross-sectional area of the nanofibrous nonwoven mat or yarn due to porosity [11]. It is therefore desirable to compare the mechanical properties of nanofibrous nonwoven mats or yarns as well as single nanofibers.

In our previous study, we have successfully prepared syndiotactic polypropylene (sPP) nanofibers from the solution using mixed and polar solvent system via solution electrospinning [12, 13]. We found that the morphologies of sPP fibers were strongly dependent on the environmental condition and solvent polarity during electrospinning, and stable form I was the dominant crystal structure in electrospun sPP fibers. However, there are few reports on the effects of organic solvent on mechanical properties of electrospun sPP nanofibers. In this article, we report the effects of organic solvents, such as decahydro naphthalene (decalin) and cyclohexane, on the tensile strength of the single sPP nanofibers as well as the nonwoven sPP nanofiber mats prepared by solution electrospinning.

Experimental

Materials

Syndiotactic polypropylene (sPP, melt index: 4.5 g/10 min at 230 °C with a load 2.16 kg, ASTM D1238) used in this study was purchased from Aldrich. The weight-average (M_w) and number-average molecular weight (M_n) are 127 and 54 kg/mol, respectively ($M_w/M_n = 2.35$). Cyclohexane, acetone, and dimethylformamide (DMF) were purchased from Aldrich. All chemicals were purchased from Wako, Japan and used without further purification.

Preparation of sPP solutions for electrospinning

In this study, two mixed solvent systems were used for solution electrospinning of sPP. One is a mixture of decahydro naphthalene (decalin), acetone, and DMF (decalin-base solvent, 80/10/10 by weight ratio) [12]. The sPP solution dissolved in the decalin-base solvent with a concentration of 12 wt% was heated up to 70 °C, and then cooled down to 40 °C for electrospinning. The other is a mixture of cyclohexane, acetone, and DMF (cyclohexane-base solvent, 80/10/10 by weight ratio) [13]. According to the similar procedure to decalin-base solvent, the sPP solution dissolved in the cyclohexane-base solvent with a concentration of 5.0 wt% was heated up to 60 °C, and then cooled down to room tempareture for electrospinning.

Electrospinning

The electrospinning of sPP solutions were carried out according to the previously reported conditions [12, 13]. In brief, the sPP solutions dissolved in decalin-base solvent were poured into a 5 mL glass syringe equipped with a 20 gauge needle. A high-voltage power supply (Har-100*12,Matsusada, Co., Japan) was used to generate a potential difference of 10 kV between the needle and an aluminum foil-covered grounded metallic rotating drum placed 15 cm from the tip of the needle. Heat gun (GHG660LCD, BOSH Co., Ltd, Germany) was used to keep temperature of a glass syringe, a metal tip, and the sPP solution at 40 °C during electrospinning. Also, the sPP solutions dissolved in cyclohexane-base solvent were poured into a 5 mL glass syringe equipped with a 21 gauge needle. Power supply was 10 kV, and the distance between the tip of the needle and an aluminum foil-covered grounded metallic rotating drum was 15 cm.

Measurements

The morphology of the electrospun sPP fibrous membranes was examined with scanning electron microscopy (SEM, VE-8800, Keyence Co., Japan). Wide-angle X-ray diffraction (WAXD) experiments were performed at room temperature with nanofiber samples using a Rotaflex RTP300 (Rigaku Co., Japan) X-ray diffractometer operating at 50 kV and 200 mA. Nickel-filtered Cu K_α radiation was used for the measurements, along with an angular range of $5 < 2\theta < 30°$. For determining the mechanical properties of single nanofibers, we specially developed the test machine (FITRON NFR-1000, RHESCA Co., Japan, [14], Fig. 1). Sample frame for collecting a single nanofiber is shown in Fig. 1. After a suitable fiber is selected and pasted with adhesive on a sample holder, the fiber axis is precisely set to align the stress axis of the holder using an optical microscopy. The fiber diameters were measured by optical microscopy with high-magnification, high-resolution zoom lens (VH-Z500R, N.A. of 0.82, up to 5000× magnification with a 4.4 mm working distance). The main specifications of the developed system are as follows: the maximum loading capacity: 500 mN, the stroke: 20 mm, the loading speed: 5–20 μm/s, the displacement sensitivity: 1.0 μm, loading sensitivity: 1.0 μN. Three parameters were determined from each stress–strain curve: Young’s modulus, tensile strength, and elongation at break. The detailed characteristics were described in Table 1. Mechanical properties of electrospun sPP nanofiber webs were determined with a universal testing machine (UTM, AG-5000G, Shimadzu, Japan) under a crosshead speed 10 mm/min at room temperature. All samples were prepared in the form of standard dumbbell-shaped according to ASTM D638 by die cutting from electrospun sPP fabrications.

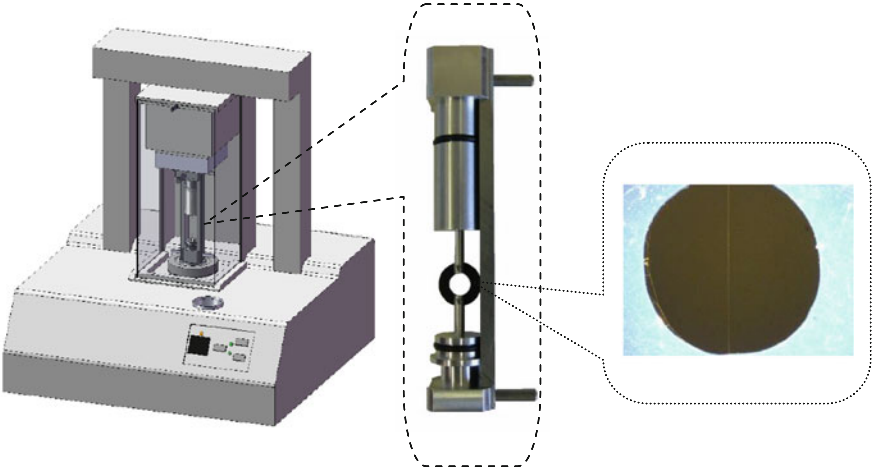

Fig. 1 Specially developed tensile test machine, sample frame for collecting a single nanofiber, and holder unit

Table 1 Mechanical properties of both electrospun sPP single nanofibers and nonwoven sPP nanofiber mats prepared from decalin-base and cyclohexane-base solutions, respectively

		Young's modulus (MPa)	Tensile stress (MPa)	Elongation at break (%)
Nonwoven nanofiber mats	Cyclohexane	20.0 ± 0.8	2.1 ± 0.4	77.6 ± 0.6
	Decalin	20.1 ± 0.9	4.1 ± 0.6	128.3 ± 0.5
Single nanofibers	Cyclohexane	39.1 ± 1.4	18.2 ± 1.1	46.7 ± 1.2
	Decalin	174.6 ± 1.7	61.4 ± 1.5	35.2 ± 1.7

Results and discussion

We have recently reported the mechanical properties of single nanofibers by using a developed tensile test apparatus, and demonstrated that the test machine was well operated for the measurement of mechanical properties of nano/micro-sized fibers [4, 10]. Figure 2 shows the typical stress–strain curves of the electrospun single sPP nanofibers prepared from different multicomponent solvent system, decalin-base solvent (a) and cyclohexane-base solvent (b), respectively. Compared to cyclohexane-base sPP single nanofiber, surprisingly the decalin-base sPP single nanofiber exhibited higher tensile strength (ca. 61 MPa), suggesting that the decalin-base sPP single nanofiber is stronger. The results may be caused by the difference in surface morphologies as well as in crystallinity in case of semicrystalline polymers, which can be easily understood in that the defects formed on the surface of the sPP nanofibers and the lower crystallinity make the nanofibers weakened considerably. Indeed, from the result of SEM analysis, one can notice that the cyclohexane-base sPP nanofibers showed the roughened surfaces (inset b in Fig. 2) whereas the decalin-base sPP nanofibers exhibited the smooth surfaces. This phenomenon was attributed to the result of rapid gelation in a heterogeneous system with solvent-rich and solvent-poor regions [13].

In addition, except for the morphological effects on the mechanical properties of electrospun sPP fibers, it can be considered that an increase in crystallinity brings about increases in modulus and tensile strength. The WAXD profiles of the electrospun sPP nanofiber mats prepared from (a) decalin and (b) cyclohexane-base solution is shown in Fig. 3. The decalin-base sPP nanofibers clearly showed the (200), (020), (121), and (400) crystal reflections at 2θ=12.16°, 15.8°, 20.5°, and 24.1° indicative of form I with an antichiral helical conformation, which is the most stable form [13, 15]. It was also considered as the disordered modification of form I because there was no existence of the (211) reflection at $2\theta = 18.9°$ indicative of structural order found in form I. Moreover, as seen in Fig. 3, a new broad peak centered at $2\theta = 16.3°$ (see the arrow in Fig. 3) appeared. This peak is generally observed in both forms II and III. On the other hand, the cyclohexane-base sPP nanofibers showed different WXAD patterns. First, a new strong peak of $2\theta = 16.0°$ appeared, corresponding to a typical peak of *trans*-planar mesophase [16, 17]. It indicates the formation of a small amount of mesophase with *trans*-planar conformation. Second, the 2θ value corresponding to the (200) crystal reflection was slightly changed to $2\theta = 12.16°$ (Fig. 3a) compared to the peak of cyclohexane-base sPP nanofibers ($2\theta = 12.34°$, Fig. 3b), which is not clear but may be the modification of form I due to the formation of mesophase. From these results, it was evident that surface morphologies and crystalline structures played a significant role in the tensile strength of the resultant sPP nanofibers.

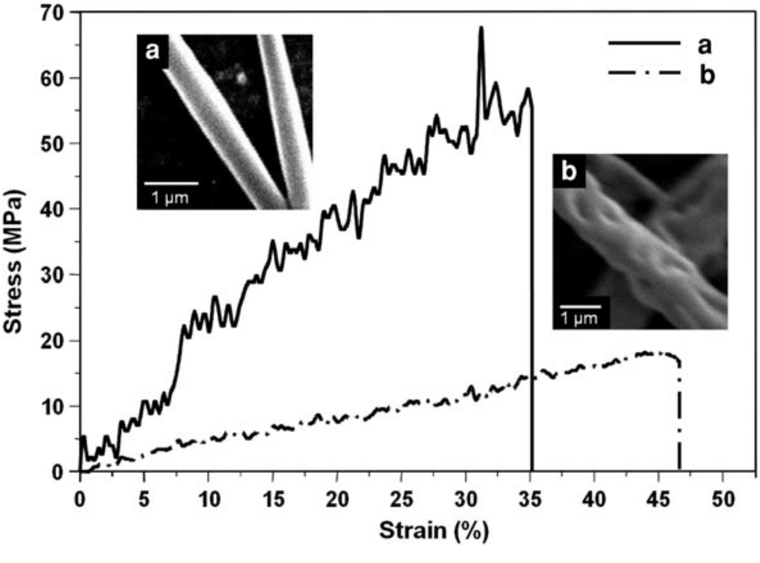

Fig. 2 Typical stress–strain curves of the electrospun sPP single nanofibers prepared from decalin (*a*) and cyclohexane (*b*) base solutions and its corresponding surface morphologies (*insets a* and *b*)

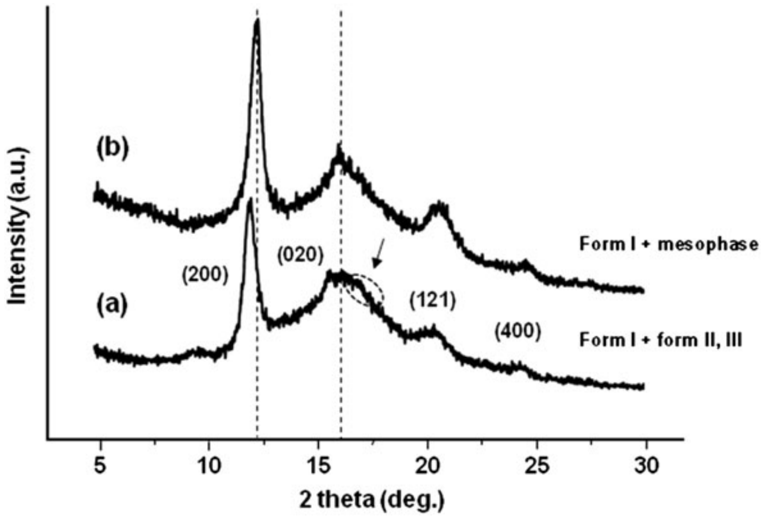

Fig. 3 WAXD profiles of the electrospun sPP nanofiber mats prepared from (*a*) decalin-base and (*b*) cyclohexane-base solutions

Furthermore, it is also useful to evaluate the tensile strength of electrospun sPP nanofiber mats in that the ultimate mat properties such as overall membrane strength (related to individual fiber strength, average fiber length, and fiber entanglement density) and porosity play an equally important role in end-use applications [5]. Figure 4 shows typical stress–strain curves of the electrospun nanofiber mats prepared from different multicomponent solvent system, decalin-base solvent (Fig. 4a) and cyclohexane-base solvent (Fig. 4b), respectively. As expected, the decalin-base sPP nonwoven mat exhibited about two times higher tensile strength (ca. 4.1 MPa) than the cyclohexane-base sPP nanwoven mat, indicating that the decalin-base sPP nonwoven mat is stronger. The results may be due to different fiber entanglement density in the electrospun fiber mats, as can be seen in SEM images (Fig. 5). Correspondingly, its elongation at break (ca. 128.3 ± 0.5%) of decalin-base sPP nonwoven mat was higher than that (ca. 77.6 ± 0.6%) of cyclohexane-base sPP nonwoven mat.

Figure 5 shows SEM images of the sPP electrospun nanofibers (electrospinning time; 20 s) prepared from decalin-base and cyclohexane-base solvents, respectively. Their average fiber diameters were 530 ± 130 nm (decalin-base) and 760 ± 370 nm (cyclohexane-base). As can be seen in Fig. 5, the coiled and dense (circular and looping) deposition of the sPP nanofibers prepared from decalin-base solution was denser than cyclohexane-base solution system, which resulted in an increased mechanical properties of the sPP nanofibers prepared from decalin-base solution. Such circular and looped fibers were commonly observed with solution electrospinning. Also, the circular and looping deposition of the electrospun fibers is an interesting phenomenon also seen with melt electrospinning [18], which may form with particularly cooled parts of the polymer jets that have a high evaporation of solvents. As seen in Fig. 5, it can be considered that such smaller coiled circular and

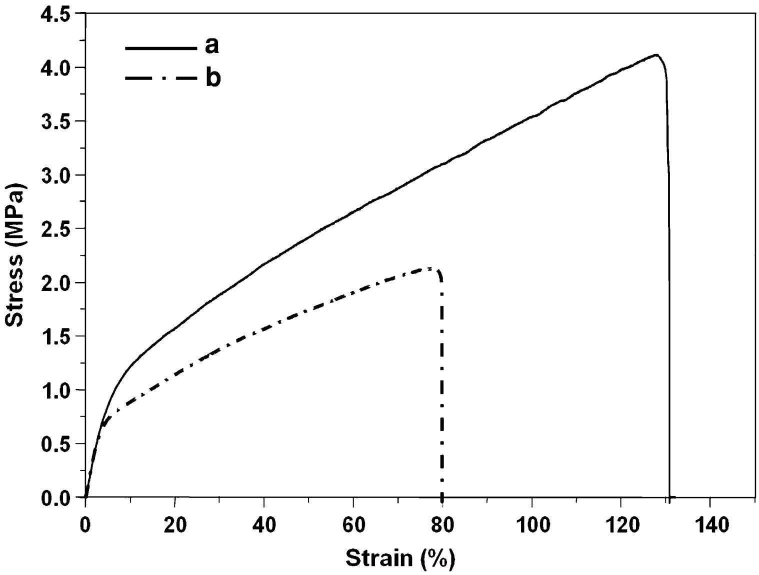

Fig. 4 Typical stress–strain curves of the electrospun sPP nanofiber mats prepared from (*a*) decalin-base and (*b*) cyclohexane-base solutions

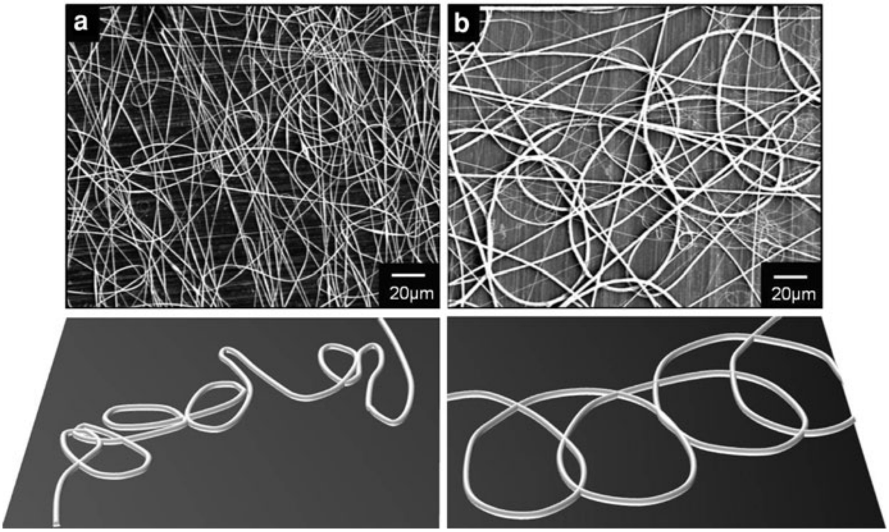

Fig. 5 SEM images and typical trajectories (cartoons in *bottom*) of commonly observed looping and coiled deposition phenomena for sPP electrospun fibers prepared from **a** decalin-base and **b** cyclohexane-base solutions

dense deposition increased the average fiber length per unit area and fiber entanglement density, and thereby resulted in an enhanced mechanical property of the sPP electrospun nanofiber mats. Furthermore, the different circular and looped fiber morphologies were observed due to the different boiling point of cyclohexane (~81 °C) and decalin (~193 °C). That is, decalin-base solvent produced the more looping morphologies (bottom in Fig. 5a), while cyclohexane-base solvent the more looped coils morphologies (bottom in Fig. 5b), suggesting that the resultant morphologies depend on the organic solvents used. It was observed that the circular and looped diameter of the nanofiber prepared from decalin-base solution was smaller than cyclohexane-base solution. Moreover, the sPP nanofiber mats prepared from decalin-base solution was denser than cyclohexane-base solution.

Conclusions

We investigated the stress–strain behaviors of the electrospun sPP single nanofibers as well as nonwoven mats. sPP was successfully electrospun from sPP solutions using two different solvents (decalin and cyclohexane) by electrospinning. The nature of organic solvents dramatically affected the surface morphologies and the circular and looping deposition of the electrospun sPP fibers. Significantly, not only the difference in morphologies but also crystal structure affected the mechanical properties of the electrospun sPP single nanofibers and nonwoven mats. As a result, it was found that the tensile strength of both electrospun sPP single nanofibers and nonwoven mats prepared from decalin-base solution was stronger than that of cyclohexane-base solution.

Acknowledgments The authors acknowledge the support of Grant-in-Aid for Global COE Program by the Ministry of Education, Culture, Sports, Science and Technology, Government of Japan.

References

1. Park JC, Ito T, Kim KO, Kim KW, Kim BS, Khil MS, Kim HY, Kim IS (2010) Electrospun poly(vinyl alcohol) nanofibers: effects of degree of hydrolysis and enhanced water stability. Polym J 42:273–276
2. Ohsawa O, Lee KH, Kim BS, Lee S, Kim IS (2010) Preparation and characterization of polyketone (PK) fibrous membrane via electrospinning. Polymer 51:2007–2012
3. Kimura N, Kim HK, Kim BS, Lee KH, Kim IS (2010) Molecular orientation and crystalline structure of aligned electrospun nylon-6 nanofibers: effect of gap size. Macromol Mater Eng 295:1090–1096
4. Watanabe K, Nakamura T, Kim BS, Enomoto Y, Kim IS (2011) Fabrication of uniaxially aligned syndiotactic polypropylene nanofibers via sample handspinning. Macromol Mater Eng 13(5): 376–382
5. Christopher JE, Alhad P, David WG, Christopher WM, Frank SB (2007) Melt blown nanofibers: fiber diameter distributions and onset of fiber breakup. Polymer 48:3306–3316
6. Grafe T, Graham K (2003) Polymeric nanofibers and nanofiber webs: a new class of nonwovens. Int Nonwovens J 12:51–55
7. Huang ZM, Zhang YZ, Kotaki M, Ramakrishna S (2003) A review on polymer nanofibers by electrospinning and their applications in nanocomposites. Compos Sci Technol 63:2223–2253
8. Zhang Y, Lim CT, Ramakrishna S, Huang ZM (2005) Recent development of polymer nanofibers for biomedical and biotechnological applications. J Mater Sci Mater Med 16:933–946
9. Zhou FL, Gong RH (2008) Manufacturing technologies of polymeric nanofibres and nanofibre yarns. Polymer Int 57:837–845
10. Kim HR, Ito T, Kim BS, Watanabe Y, Kim IS (2011) Mechanical properties, morphologies, and microstructures of novel electrospun metallized nanofibers. Adv Eng Mater 13(5):376–382

11. Wang M, Jin HJ, Kaplan DL, Rutledge GC (2004) Mechanical properties of electrospun silk fibers. Macromolecules 37:6856–6864
12. Watanabe K, Nakamura T, Kim BS, Kim IS (2011) Preparation and characteristics of electrospun polypropylene fibers: effect of organic solvents. Adv Mater Res 175–176:337–340
13. Lee KH, Ohsawa O, Watanabe K, Kim IS, Givens SR, Chase B, Rabolt JF (2009) Electrospinning of syndiotactic polypropylene from a polymer solution at ambient temperatures. Macromolecules 42:5215–5218
14. Kim IS, Enomoto Y, Takahashi T (2009) Mechanical characteristic evaluation test of ultrafiner fibers. Sen'i Gakkaishi 65:325–327
15. Auriemma F, De Rosa C (2003) Time-resolved study of the martensitic phase transition in syndiotactic polypropylene. Macromolecules 36:9396–9410
16. Zhang X, Li R, Kong L, Wang D (2008) Stress-induced structure transition of syndiotactic propylene via melt spinning. Polymer 49:1350–1355
17. De Rosa C, Auriemma F (2006) Structure and physical properties of syndiotactic polypropylene: a highly crystalline thermoplastic elastomers. Prog Polym Sci 31:145–237
18. Dalton PD, Grafahrend D, Klinkhammer K, Klee D, Möller M (2007) Electrospinning of polymer melts: phenomenological observations. Polymer 48:6823–6833